



# HOKKAIDO UNIVERSITY

Title	Thermogravimetric analysis and microstructural observations on the formation of GaN from the reaction between Ga <sub>2</sub> O <sub>3</sub> and NH <sub>3</sub>
Author(s)	Kiyono, Hajime; Sakai, Toshiki; Takahashi, Mari et al.
Citation	Journal of Crystal Growth, 312(19), 2823-2827 <a href="https://doi.org/10.1016/j.jcrysgr.2010.06.021">https://doi.org/10.1016/j.jcrysgr.2010.06.021</a>
Issue Date	2010-09-15
Doc URL	<a href="https://hdl.handle.net/2115/44033">https://hdl.handle.net/2115/44033</a>
Type	journal article
File Information	JCG312-19_2823-2827.pdf



**Thermogravimetric analysis and microstructural observations on the formation of GaN from the reaction between Ga<sub>2</sub>O<sub>3</sub> and NH<sub>3</sub>**

**Hajime Kiyono\*, Toshiki Sakai, Mari Takahashi, and Shiro Shimada  
Graduate School of Engineering, Hokkaido University, Sapporo, 060-8628, JAPAN**

**Abstract**

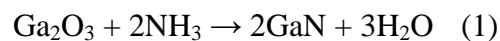
Thermogravimetric analysis (TGA) and microstructural observations were carried to investigate the nitridation mechanism of  $\beta$ -Ga<sub>2</sub>O<sub>3</sub> powder to GaN under an NH<sub>3</sub>/Ar atmosphere. Non-isothermal TGA showed that nitridation of  $\beta$ -Ga<sub>2</sub>O<sub>3</sub> starts at ~650 °C, followed by decomposition of GaN at ~1100 °C. Isothermal TGA showed that nitridation follows linear kinetics in the temperature range 800–1000 °C. At an early stage of nitridation, small GaN particles (~5 nm) are deposited on the  $\beta$ -Ga<sub>2</sub>O<sub>3</sub> crystal surface, and they increase with time. We proposed a mechanism for the nitridation of Ga<sub>2</sub>O<sub>3</sub> by NH<sub>3</sub> whereby nitridation of  $\beta$ -Ga<sub>2</sub>O<sub>3</sub> proceeds via the intermediate vapor species Ga<sub>2</sub>O (g).

Keywords: A1, Growth models, A2. Growth from vapor, B1. Nitrides

PACS: 81.10.St Growth in controlled gaseous atmospheres

## 1. Introduction

Gallium nitride (GaN) is a promising wide-band gap semiconductor used in manufacturing light emitting diodes, laser diodes, and ultra-violet photo detectors. [1–3] GaN epilayers are usually fabricated by chemical vapor deposition using metal-organic gallium compounds. In general, such metal-organic compounds are expensive and difficult to handle in air, another method to fabricate GaN has been needed. It has been reported that GaN powders can be also prepared by nitridation of Ga<sub>2</sub>O<sub>3</sub> by NH<sub>3</sub>. [4–7] Recently, GaN epilayers, nanotubes, and nanobelts have been produced by this method. [8–11] In addition, bulk GaN crystals have been synthesized by carbothermal reduction and nitridation of  $\beta$ -Ga<sub>2</sub>O<sub>3</sub> by NH<sub>3</sub>. [12–15] These results indicate that the nitridation of Ga<sub>2</sub>O<sub>3</sub> by NH<sub>3</sub> is an important method for fabricating GaN materials. The overall reaction for nitridation of Ga<sub>2</sub>O<sub>3</sub> by NH<sub>3</sub> is as follows:



Balkas et al. pointed out, on the basis of thermodynamic calculations, that reaction (1) does not occur directly but rather through intermediate gaseous species of Ga<sub>2</sub>O (g). They suggested that GaN is formed by the reaction between NH<sub>3</sub> and the gaseous Ga<sub>2</sub>O. [6] Luo et al. also suggested the formation of gaseous Ga<sub>2</sub>O as an intermediate species by reaction

between  $\beta$ -Ga<sub>2</sub>O<sub>3</sub> and H-containing species that are formed by thermal decomposition of NH<sub>3</sub>. Jung et al. suggested the nitridation of  $\beta$ -Ga<sub>2</sub>O<sub>3</sub> by NH<sub>3</sub> proceeds via solid state species such as GaO<sub>x</sub>N<sub>y</sub> (s). [16, 17] From the previous studies, it can be concluded that the mechanism of Ga<sub>2</sub>O<sub>3</sub> nitridation by NH<sub>3</sub> is still not clear. Usually, the kinetics of a chemical reaction provides information about its mechanism. The present study investigates the nitridation of  $\beta$ -Ga<sub>2</sub>O<sub>3</sub> to GaN by NH<sub>3</sub> on the basis of kinetic results using thermogravimetric analysis (TGA) and microstructural observations; a nitridation mechanism is proposed.

## 2. Experimental procedures

### 2.1 $\beta$ -Ga<sub>2</sub>O<sub>3</sub> powder

Commercially available  $\beta$ -Ga<sub>2</sub>O<sub>3</sub> powder (99.9% purity; Koujyundo Kagaku Co.) was used for the nitridation. Figure 1(a) shows the scanning electron microscopic (SEM) images of as-received  $\beta$ -Ga<sub>2</sub>O<sub>3</sub> powder. The powder contains secondary particles about 1–10  $\mu$ m long consisting of primary particles of about 0.1  $\mu$ m in size. When as-received  $\beta$ -Ga<sub>2</sub>O<sub>3</sub> powder was sintered at 1400 °C for 1 h in Ar,  $\beta$ -Ga<sub>2</sub>O<sub>3</sub> powders were coarsened as a result of the growth of primary particles, accompanied by diminishing pore size (Fig. 1 (b)). The secondary particle sizes were almost same as those of the as-received powder. The sintered powder was also used for the nitridation. The specific surface area of the as-received and

coarse  $\beta$ -Ga<sub>2</sub>O<sub>3</sub> powder was about 10 and 1 m<sup>2</sup>/g, respectively, as measured by the BET method using N<sub>2</sub> gas (BELSORP-mini, BEL JAPAN,).

## ***2.2 Thermogravimetric analysis and microstructural observations***

The weight change during nitridation was continuously monitored by an electric micro balance (Cahn D200). The  $\beta$ -Ga<sub>2</sub>O<sub>3</sub> powder was placed in an alumina cell, which was hung with alumina wires with about 40 cm long in total and located in a fused quartz tube in a vertical furnace. Mixed gases of NH<sub>3</sub>/Ar (10/90, 50/50, 90/10 kPa), H<sub>2</sub>/Ar (40/60 kPa), or Ar (100 kPa) at a total flow rate of 100 mL/min were introduced at the top of the tube. Non-isothermal nitridation was carried out by heating  $\beta$ -Ga<sub>2</sub>O<sub>3</sub> to 1200 °C at a rate of 5 °C /min, while isothermal nitridation was carried out at a temperature 800–1000 °C for about 1 h. In the non-isothermal nitridation, the exhaust gas from the TG system was analyzed by a mass-spectrometer (VG GAS ANALYZER, FISON). The sampling point of the exhaust gas was about 20 cm downstream from the sample holder, where the gas was cooled to room temperature. The nitrated samples from both non-isothermal and isothermal TGA were characterized by X-ray powder diffraction (XRD, RINT 2000, RIGAKU), SEM (JSM-6300F, JEOL), and high-resolution TEM-SEM (HD-2000, HITACHI). The residual oxygen in the sample was determined using an oxygen and nitrogen analyzer (EMGA-620W, HORIBA).

### 3. Results and Discussion

#### 3.1 The results of thermogravimetric analysis

Non-isothermal TGA results of as-received  $\beta$ -Ga<sub>2</sub>O<sub>3</sub> powder obtained by heating to 1200 °C in NH<sub>3</sub>/Ar (50/50 kPa), H<sub>2</sub>/Ar (40/60 kPa), and Ar atmospheres are shown in Fig. 2. No weight change was observed in the Ar atmosphere over the entire temperature range (20–1200 °C); suggesting that vaporization of  $\beta$ -Ga<sub>2</sub>O<sub>3</sub> powder does not occur in that temperature range. In H<sub>2</sub>/Ar (40/60 kPa), the weight loss starts at ~800 °C. On the basis of thermodynamic calculations, Butto et al. suggested that Ga<sub>2</sub>O (g) is formed as a main product above 720 °C by the reaction between Ga<sub>2</sub>O<sub>3</sub>(s) and H<sub>2</sub> given as follows:[18]



Apparently, the weight loss in an H<sub>2</sub>/Ar atmosphere is caused by the generation of Ga<sub>2</sub>O (g) by partial decomposition or reduction of  $\beta$ -Ga<sub>2</sub>O<sub>3</sub>. In NH<sub>3</sub>/Ar (50/50 kPa), the weight loss starts at ~650 °C and decreases to ~10 wt%, reaching a short plateau at ~870°C (first weight loss). After the plateau, the weight decreases further, starting around 1000 °C, and becomes significant above 1100 °C (second weight loss). Figure 3 shows the XRD patterns for as-received  $\beta$ -Ga<sub>2</sub>O<sub>3</sub> powder and for the sample heated to 870 °C and 1200 °C in Ar/NH<sub>3</sub> (50/50 kPa). This indicates that  $\beta$ -Ga<sub>2</sub>O<sub>3</sub> begins to change to a wurtzite-type GaN above 870 °C,

the latter becoming well-crystallized at 1200 °C. The weight loss due to the complete nitridation of  $\beta$ -Ga<sub>2</sub>O<sub>3</sub> to GaN in Eq (1) is calculated to be -10.6%. A relatively good agreement between the first weight loss and the calculated one for the complete nitridation showed that the first weight loss is caused by the complete nitridation of  $\beta$ -Ga<sub>2</sub>O<sub>3</sub> to GaN. The second weight loss after the plateau (>1000 °C) resulted from decomposition of GaN in NH<sub>3</sub>. In the non-isothermal experiment in NH<sub>3</sub>/Ar and H<sub>2</sub>/Ar atmospheres, gas species containing Ga (> 69.7 in mass number) in the exhaust gas were not detected by the mass-spectroscopic analysis.

The kinetic results by isothermal TGA for the nitridation of as-received  $\beta$ -Ga<sub>2</sub>O<sub>3</sub> powder in the temperature range 800–1000 °C are shown in Fig. 4. After the TG analysis, no deposit was observed at the outside wall of sample cell, hanging wires or inner wall of a furnace tube. Over this temperature range, the weight loss from -1% to -9% occurs linearly with time (dashed lines). The samples obtained at the weight loss of -10% over the entire temperature range gave only GaN peaks on XRD, indicating the nitridation of  $\beta$ -Ga<sub>2</sub>O<sub>3</sub> by NH<sub>3</sub> according to Eq (1). The close-to-linear weight loss curve suggests that the nitridation is limited by an interfacial reaction.

$$\Delta W / W_{\text{theo}} \times 100 = kt \quad (3)$$

where,  $\Delta W$  is the observed weight loss,  $W_{\text{theo}}$  the theoretical weight loss when the nitridation is completed (-10.6%),  $k$  the rate constant, and  $t$  the reaction time. From the slope of the linear region,  $k$  was calculated at each temperature. The Arrhenius plots of the  $k$  value provide activation energy of 110 kJ mol<sup>-1</sup> for nitridation reaction. The weight loss reduced after -9%, barely approaching the theoretical weight loss (-10.6%) due to the characteristic of complete nitridation. The sample obtained after the isothermal nitridation at 1000 °C actually contained about 4 wt% oxygen, suggesting the difficulty in complete removal of oxygen.

Figure 5(a) shows the weight loss by nitridation of  $\beta$ -Ga<sub>2</sub>O<sub>3</sub> at various  $P_{\text{NH}_3}$  at 800 °C. These results indicate that the weight loss proceeds linearly to -8% ~ -10.8 %. The nitridation rate constant was calculated from the slope of the straight line approximation of the curves. A linear relationship exists between the rate constants and  $P_{\text{NH}_3}$  (Fig. 5(b)). The nitridation of as-received and coarse  $\beta$ -Ga<sub>2</sub>O<sub>3</sub> powders measured by isothermal TGA at 800 °C was compared (Fig. 6). At an early stage (0% to -3%), the nitridation rate for coarse  $\beta$ -Ga<sub>2</sub>O<sub>3</sub> powder was slower than that of the as-received one; however, the two were almost the same at a middle stage (-3% to -8%). The surface area of the as-received  $\beta$ -Ga<sub>2</sub>O<sub>3</sub> powder was about ten times larger than that of the coarse powder, hence the slower rates for the coarsened

sample at the early stage is because of its smaller surface area.

### ***3.2 Microstructural observation***

Figure 7 shows SEM photographs of coarse  $\beta$ -Ga<sub>2</sub>O<sub>3</sub> particles nitrated at various weight losses. The un-nitrated coarse  $\beta$ -Ga<sub>2</sub>O<sub>3</sub> particles have a smooth surface with stepped hexagonal plates (Figs. 7 (a) and (a')). At -0.3% weight loss, very small particles (~5 nm) are formed on the surface of the coarse  $\beta$ -Ga<sub>2</sub>O<sub>3</sub> particles (Figs. 7 (b) and (b')); the number and size of these particles on the coarse  $\beta$ -Ga<sub>2</sub>O<sub>3</sub> increases with nitridation (Figs. 7(c)–(f)). Since the samples of -1.8 to -8.1% weight loss exhibited the GaN peaks in XRD, the deposited particles must be GaN. At -5.8 and -8.1% weight loss, the triangle rectangular particles are piled up on sloughs of Ga<sub>2</sub>O<sub>3</sub>, forming hollow or tubular aggregates GaN (Figs. 7(e) and (f)).

### ***3.4 Nitridation mechanism***

We propose, based on the kinetic results and microstructural observations, a nitridation mechanism consisting of four steps as shown in Fig. 8, in the temperature range of 800–1000 °C. First, Ga<sub>2</sub>O (g) is formed by the reaction between  $\beta$ -Ga<sub>2</sub>O<sub>3</sub> (s) and H<sub>2</sub> and/or H-containing reactive species formed by the thermal decomposition of NH<sub>3</sub> (Fig. 8 (a)). NH<sub>3</sub> is mostly decomposed to H<sub>2</sub> and N<sub>2</sub> at ~1000 °C under equilibrium conditions; however, a

previous study found that the decomposition of NH<sub>3</sub> was about 10% or lower at around 1000 °C in an open flow system.[19] Other studies suggest that some reactive intermediate species, such as H, NH, or NH<sub>2</sub> radicals, are formed during the thermal decomposition of NH<sub>3</sub>. [6, 8] From non-isothermal TG results (Fig. 2), decomposition of  $\beta$ -Ga<sub>2</sub>O<sub>3</sub> to Ga<sub>2</sub>O(g) by H<sub>2</sub> (eq. 2) in an H<sub>2</sub>/Ar (40/60 kPa) atmosphere starts above 800 °C, showing that H<sub>2</sub> and/or the reactive intermediate species containing H formed by thermal decomposition of NH<sub>3</sub> can react with  $\beta$ -Ga<sub>2</sub>O<sub>3</sub> (s) to form Ga<sub>2</sub>O (g). In the second step (Fig. 8 (b)), Ga<sub>2</sub>O (g) reacts with NH<sub>3</sub> resulting in the deposition of nano-sized GaN particles on surface of the  $\beta$ -Ga<sub>2</sub>O<sub>3</sub> particles given as follows:



The reaction (Eq. (4)) controls the nitridation of  $\beta$ -Ga<sub>2</sub>O<sub>3</sub>, as shown in Figs. 4 and 5, because the nitridation proceeds linearly with time and the nitridation rate depends linearly on  $P(\text{NH}_3)$ .

As nitridation progresses, the number and size of deposited GaN particles increases with the coagulated particles. At the third step (Fig. 8 (c)), such coagulated GaN particles are in triangular and rectangular shapes covering the starting  $\beta$ -Ga<sub>2</sub>O<sub>3</sub> particles. H<sub>2</sub> and/or H-containing species are free to move into a Ga<sub>2</sub>O<sub>3</sub> particle through GaN walls to form Ga<sub>2</sub>O (g); however, the gas is confined inside GaN walls leading to an increase in the internal

pressure. As a result of  $\text{Ga}_2\text{O}$  (g) escaping, the GaN forms tubes or hollows (Fig. 8 (d)). Once an exit is created, the reaction (Eq. (4)) proceeds linearly in proportion to  $P(\text{NH}_3)$ . In this reaction sequence,  $\text{Ga}_2\text{O}$  is supposed to be instable at room temperature or to be transported in short distance, because gas species containing Ga was not detected in exhaust gas of TG system.

#### 4. Summary

The kinetics of nitridation of  $\beta\text{-Ga}_2\text{O}_3$  to wurtzite-type GaN in an  $\text{NH}_3/\text{Ar}$  atmosphere was studied by TGA and microstructural observation. Non-isothermal TGA, nitridation of  $\beta\text{-Ga}_2\text{O}_3$  started at  $\sim 650$  °C; followed by the decomposition of GaN at  $\sim 1100$  °C. The kinetic results by isothermal TGA showed that the nitridation of  $\text{Ga}_2\text{O}_3$  follows linear kinetics; suggesting that the rate-limiting step is an interfacial reaction. From microstructural observation, it was observed that nano-sized GaN particles were deposited on the surface  $\beta\text{-Ga}_2\text{O}_3$  in an early stage, which increased with time, and that the coagulated GaN particles cover the  $\text{Ga}_2\text{O}_3$  particles. We speculate that the reaction of  $\beta\text{-Ga}_2\text{O}_3$  with  $\text{H}_2$  and/or H containing species gas from  $\text{NH}_3$  produces  $\text{Ga}_2\text{O}$  (g); the latter reacts with  $\text{NH}_3$  to form GaN.

Acknowledgment

This work was supported in part by the Global COE Program (Project No. B01: Catalysis as the Basis for Innovation in Materials Science) from the Ministry of Education, Culture, Sports, Science and Technology, Japan)

## References

- [1] R. P. Vaudo, D. Goepfert, T. D. Moustakas, D. M. Beyea, T. J. Frey and K. Meehan, *J. Appl. Phys.*, **79**(1996) 2779-2783.
- [2] G. Jacob and D. Bois, *Appl. Phys. Lett.*, **30** (1977) 412-414.
- [3] S. J. Pearton and F. Ren, *Advanced Materials*, **12** (2000)1571.
- [4] A. Addamiano, *J. Electrochem. Soc.*, **108** (1961) 1072-1072.
- [5] B. B. Binkowski and M. R. Lorent, *J. Electrochem. Soc.*, **109** (1962) 24-26.
- [6] C. M. Balkas and R. F. Davis, *J. Am. Ceram. Soc.*, **79**[9] (1996) 2309-2312.
- [7] H. D. Xiao, H. L. Ma, C. S. Xue, J. Ma, F. J. Zong, X. J. Zhang, F. Ji and W. R. Hu, *Mater. Chem. Phys.*, **88** (2004) 180-184.
- [8] L. Q. Luo, K. Yu, Z. Q. Zhu, Y. S. Zhang, H. L. Ma, C. S. Xue, Y. G. Yang and S. Q. Chen, *Mater. Lett.*, **58** (2004)2893-2896.
- [9] S. Ohira, M. Yoshioka, T. Sugawara, K. Nakajima and T. Shishido, *Thin Solid Films*, **496** (2006) 53-57.
- [10] J. Dinesh, M. Eswaramoorthy and C. N. R. Rao, *J. Phys. Chem. C*, **111** (2007) 510-513.
- [11] H. J. Lee, T. I. Shin and D. H. Yoon, *Surf. Coat. Tech.*, **202** (2008) 5497-5500.
- [12] S. Shimada and R. Taniguchi, *J. Cryst. Growth*, **263** (2004)1-3.

- [13] S. Shimada, Y. Miura, A. Miura and T. Sekiguchi, *T. Cryst. Growth. Des.*, **7** (2007) 1251-1255.
- [14] A. Miura, S. Shimada, M. Yokoyama, H. Tachikawa and T. Kitamura, *Chem. Phys. Lett.*, **451** (2008) 222-225.
- [15] A. Miura, S. Shimada, T. Sekiguchi, M. Yokoyama and B. Mizobuchi, *B. J. Cryst. Growth*, **310** (2008) 530-535.
- [16] W. S. Jung, *Mater Lett*, **60** (2006) 2954-2957.
- [17] W. S. Jung, O. H. Han and S. A. Chae, *Mater. Chem. Phys.*, **100** (2006) 199-202.
- [18] D. P. Butt, Y. Park and T. N. Taylor, *J. Nucl. Mater.*, **264** (1999) 71-77.
- [19] H. Lee and J. S. Harris, *J. Cryst. Growth*, **169** (1996) 689-696.

Figures captions

Fig. 1. SEM photographs of (a) as-received and (b) coarse  $\beta$ -Ga<sub>2</sub>O<sub>3</sub> powder. The coarsened sample was fabricated by heating as-received sample at 1400 °C for 1 h. Insets are magnified images.

Fig. 2. Non-isothermal TGA curves of as-received  $\beta$ -Ga<sub>2</sub>O<sub>3</sub> powder against temperature in NH<sub>3</sub>/Ar, H<sub>2</sub>/Ar, and Ar atmospheres.

Fig. 3. XRD patterns of (a) as-received  $\beta$ -Ga<sub>2</sub>O<sub>3</sub> and the sample obtained by non-isothermal nitridation up to (b) 870 °C and (c) 1200 °C.

Fig. 4. TGA curves obtained by isothermal experiments of  $\beta$ -Ga<sub>2</sub>O<sub>3</sub> in Ar/NH<sub>3</sub> (50/50) atmosphere at the temperatures of (a) 800 °C, (b) 900 °C, and (c) 1000 °C. Dashed lines superimposed on the TGA curves show the slope of each curve. A horizontal dotted line shows the calculated weight loss based on the complete nitridation of  $\beta$ -Ga<sub>2</sub>O<sub>3</sub>.

Fig. 5. (a) Isothermal TGA curves of the fine sample at 800 °C at various  $P(\text{NH}_3)$ . Dashed

lines superimposed on the TGA curves show the slope of the each curve, and the horizontal dotted line, theoretical weight loss. (b) Plots of rate constants obtained from TGA results as a function of  $P_{\text{NH}_3}$ .

Fig. 6. Comparison of isothermal TGA curves between (a) as-received and (b) coarse  $\beta$ - $\text{Ga}_2\text{O}_3$  powder at 800 °C in Ar/ $\text{NH}_3$  atmosphere. Dashed lines superimposed on the TGA curves show the slope of each curve. The horizontal dotted line shows the calculated weight loss based on the complete nitridation of  $\text{Ga}_2\text{O}_3$ .

Fig. 7. SEM photographs of partially nitrided coarse  $\beta$ - $\text{Ga}_2\text{O}_3$  powder at 800 °C. Weight changes of the partially nitrided samples are (a) 0%, (b) -0.3%, (c) -1.8%, (d) -3.5%, (e) -5.8%, and (f) -8.1%; (a'), (b'), and (f') are magnified images of (a), (b), and (f), respectively.

Fig. 8. A model for formation of GaN from  $\beta$ - $\text{Ga}_2\text{O}_3$  in an  $\text{NH}_3$  atmosphere: (a) formation of  $\text{Ga}_2\text{O}$  (g), (b) formation of GaN depositions on  $\beta$ - $\text{Ga}_2\text{O}_3$ ; (c) growth of GaN; and (d) formation of hollow or tubular GaN aggregates.

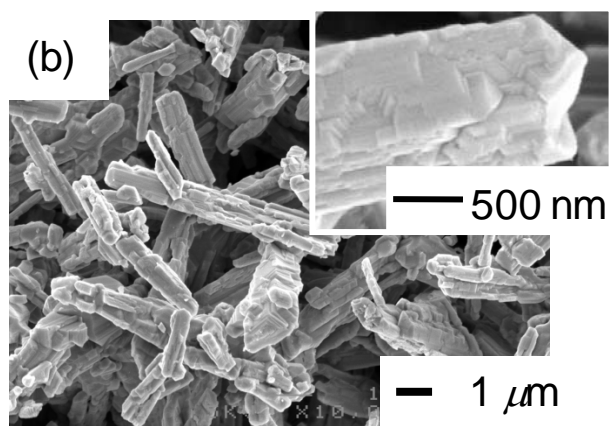
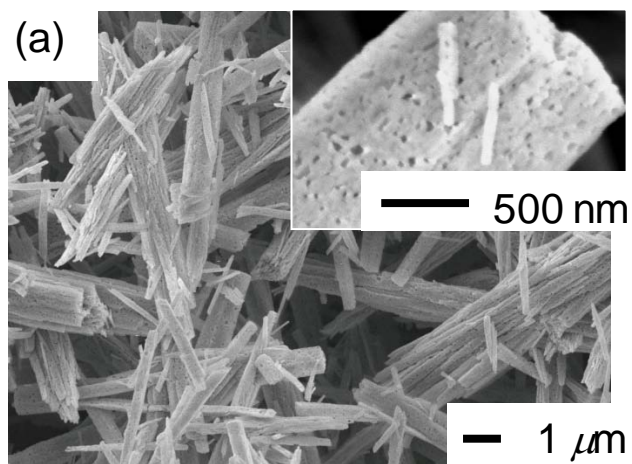


Fig. 1

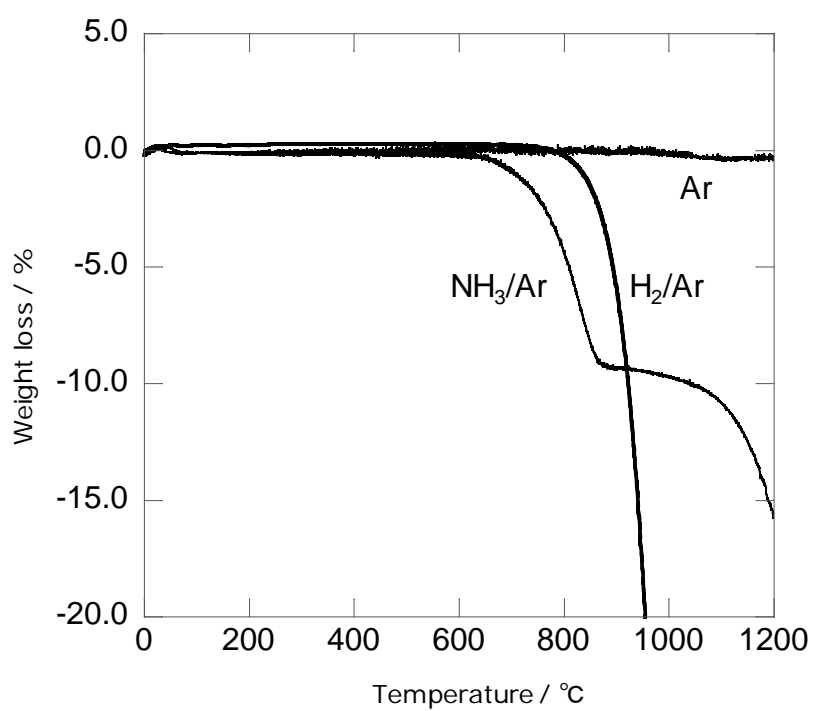


Fig.2

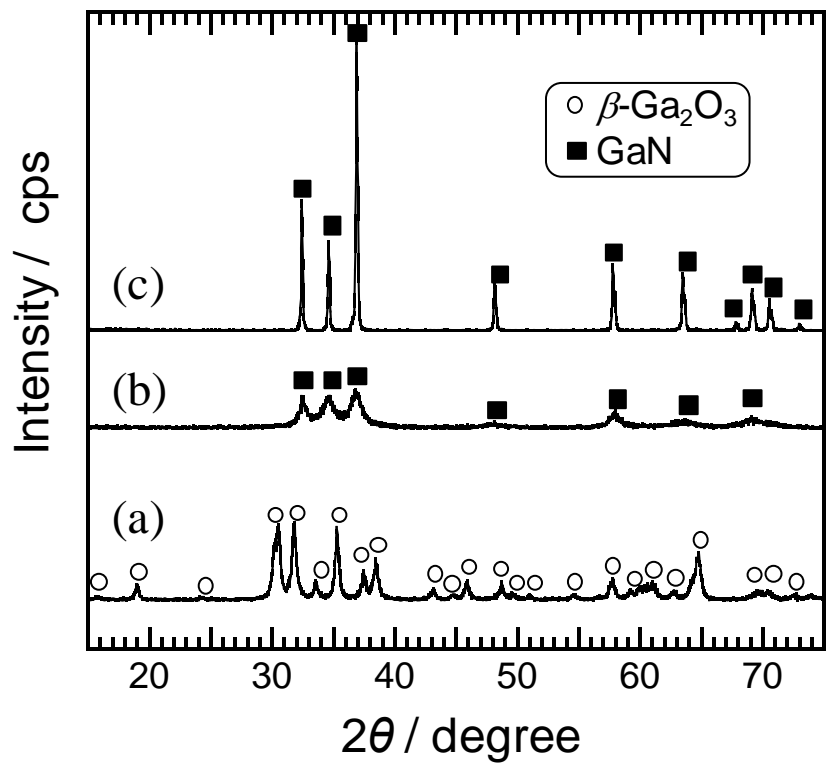


Fig.3

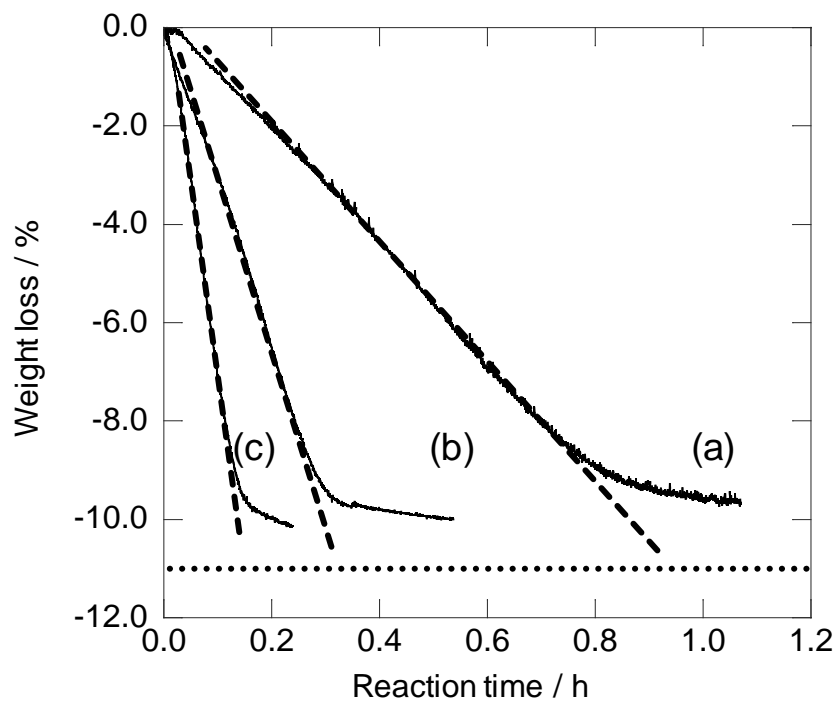


Fig.4

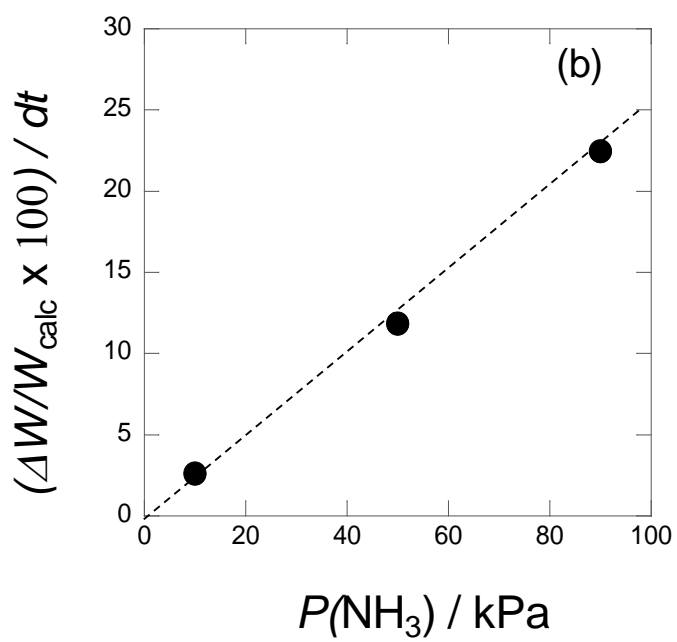
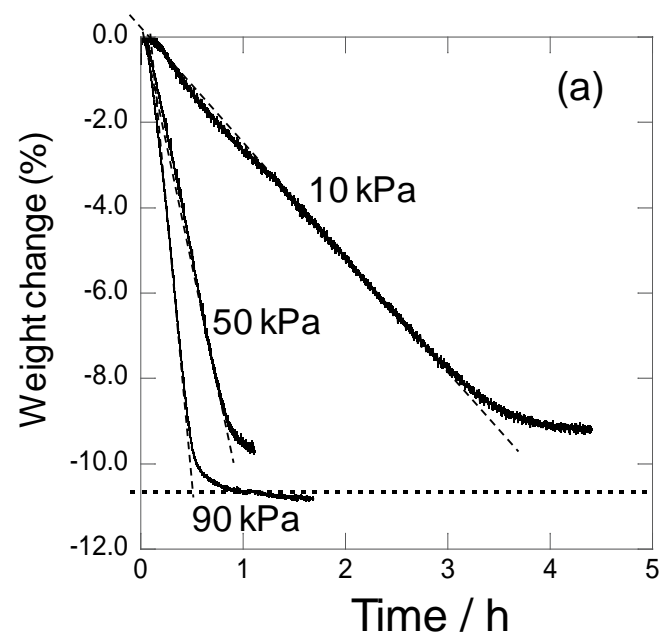


Fig.5

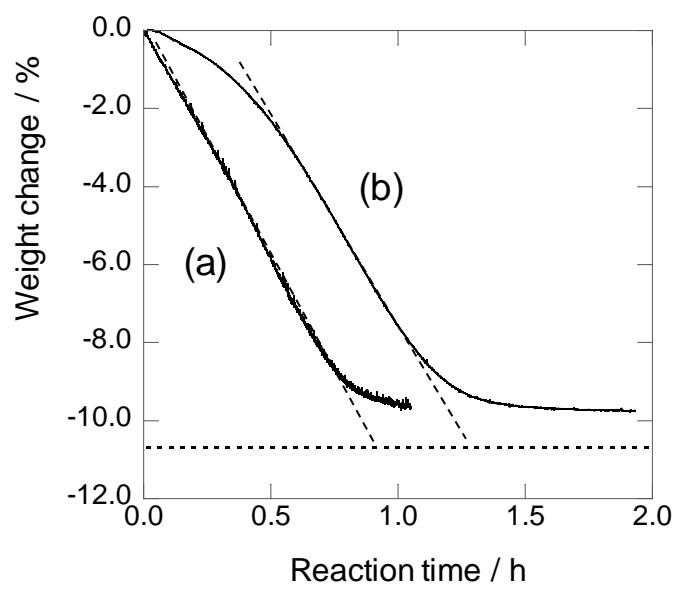


Fig.6

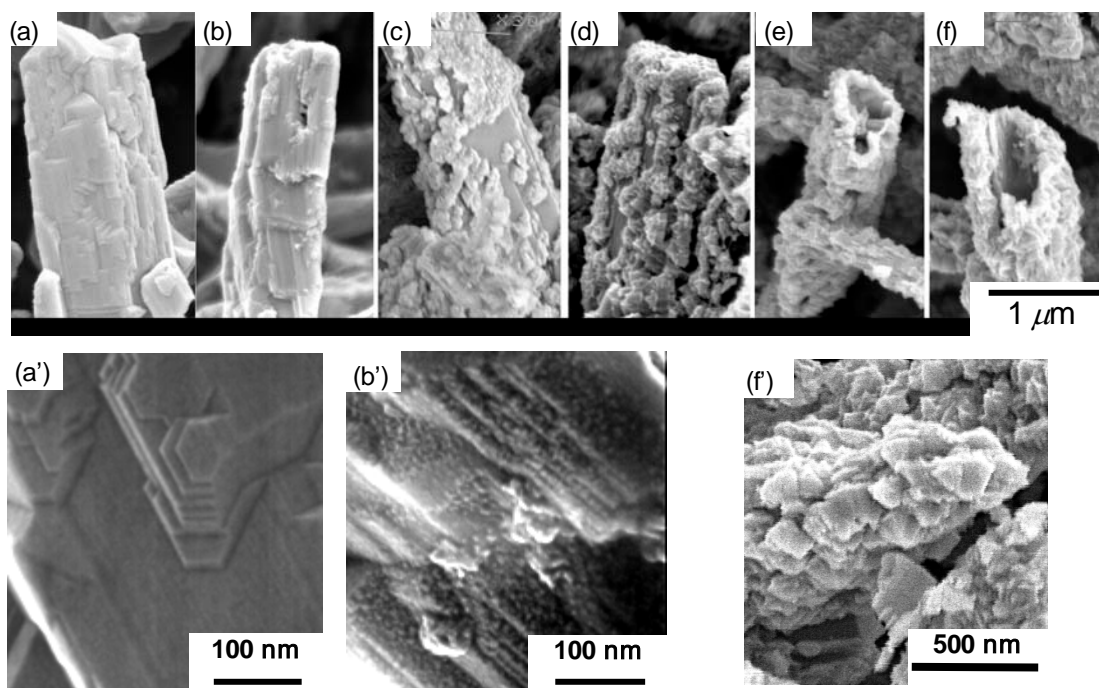


Fig.7

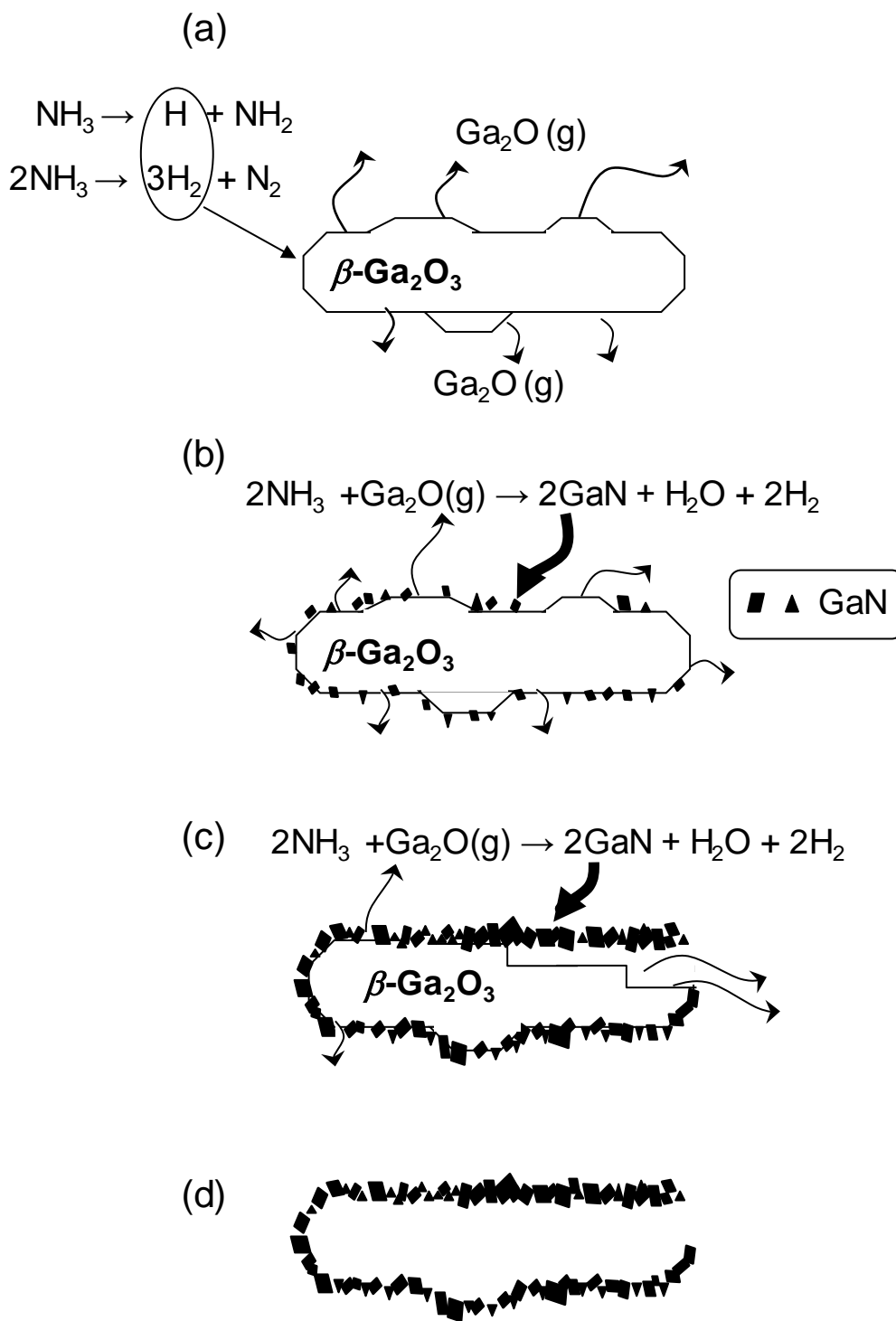


Fig.8